



Original Article

Study and experimental prototyping of a digital instrument for detection and acquisition with local monitoring on LCD of ionizing radiations using BG51 module and ESP32 microchip

Sandrine Emvoutou Ndongo^{a*}, Jean Mbihi^a, Jacquie Thérèse Ngo Bissé^b, Célestine Nguemgne Malongte^c

^aLaboratory of Research in Computer and Automatic Engineering, ENSET, University of Douala, Douala, Cameroon

^bHigher Technical Teachers Training College of University of Yaoundé I in Ebolowa, Department of maintenance, Cameroon

^cDepartment of Radiology and Medical Imaging, Douala General Hospital, Cameroon

ARTICLE INFO

Article history:

Received 26 September 2021

Revised 11 November 2021

Accepted 18 November 2021

Keywords:

Ionizing radiation;

Biomedical instrument;

BG51 sensor;

ESP32;

TFT LCD display;

medical imaging.

ABSTRACT

This paper presents a novel digital device for ionizing radiation detection in biomedical imaging media. It is designed and built using emerging technologies, in order to provide lower cost and high performance compared to existing biomedical instruments. The BG51 modular sensor is used as an ionizing radiation detector with corresponding pulses as output. Then, the ESP32 microchip acquires and digitalizes the ionizing radiation doses, and an associated 2.4-inch TFT LCD screen, is used as a hardware graphical monitor. A number of real time tests conducted in the laboratory, indicates that the ionizing radiation detection process, varies in the range [10 μ Sv 2mSv]. In addition, the sample size with rate 30 samples per second, is approximately 25 000. Furthermore, the experimental results show the graph of ionizing radiation doses within a real environment where the proposed biomedical instrument is located.

1. Introduction

The use of ionizing radiation in medicine has obvious advantages, but it is also associated with very harmful risks. These risks are caused by the radioactive products emitted by medical imaging equipment, which has the particularity of emitting ionizing radiation [1-2]. Ionizing radiation is particularly dangerous for humans for three reasons: it ionizes matter, i.e., it tears electrons from atoms during its journey; it causes electron diffusion or free radicals which can interact with the cell's DNA and cause it to break in various ways; it breaks hydrogen bonds and single or double-strand breaks, thus causing cancer [3-4-5]. Thus, ionizing radiation has an action, often negative, on the living matter [6-7]. Unlike light rays or radio waves, they are penetrating. They are not detected by the human sensory organs [8-9] which also distinguishes them from light, heat, or noise. For these reasons, a set of techniques has been developed to protect against ionizing radiation

within governmental and international commissions called radiation protection [10]. In Cameroon, for example, the National Radiation Protection Agency (ANRP) is responsible for protecting people, property, and the environment from the harmful effects of ionizing radiation [11]. It records data on the dosimetry of the environment and professional environments. Despite this, there is a lack of continuous monitoring of radiological health personnel on the systematic measurement of the level of radiation they are exposed to [12]. This is usually due to a lack of adequate equipment and a lack of professional maintenance staff [13]. However, several scientific works in the literature present accessible and convenient tools that can be tropicalized for hospitals in Cameroon. In [14], different models of gowns recommended for medical imaging rooms are proposed while [15] proposes safety procedures for the installation, use, and control of x-ray equipment in large

* Corresponding author.

E-mail address: sandrineemvoutou479@yahoo.com

Peer review under responsibility of University of El Oued.

2716-9227/© 2021 The Authors. Published by University of El Oued. This is an open access article under the CC BY-NC license

(<https://creativecommons.org/licenses/by-nc/4.0/>).

<http://dx.doi.org/10.5281/zenodo.5717122>

medical radiological facilities. The works of [16-17] and [18] present the different personal dosimeters and topographical counters used in medical radiological facilities to measure and evaluate the radiation doses absorbed by the imaging staff on duty. This technology is the most widely used, unfortunately, the dose assessment is not in real-time; it is done after a period (usually a few weeks). In addition, the device must be sent to a specialized laboratory for approximate analysis of the dose rates received, hence its limitation [19]. The studies in [20] propose a modern measuring device with 3G Ethernet or Wi-Fi internet communication including a Geiger-Müller tube. Given the lack of equipment in Cameroon and the technologies proposed in the literature, we propose a tool for local measurement of ionizing radiation that considers: the permissible level of ionizing radiation by always alerting health personnel; the portability, miniaturization of the prototype, and reduction of the acquisition cost. The present study is structured as follows. Section 2 describes the data acquisition and communication procedure at the measurement site of our work as well as the different technologies used for implementation; the third section presents the tools and methods as well as the algorithms and design architecture of the communication interface. The third section is reserved for the presentation of the results, analysis, and discussions. Finally, the last section is reserved for the conclusion and some possible innovations.

2. Tools and methodologies

2.1. Tools

Fig. 1 shows the design flowchart of the proposed airborne ionizing radiation measuring device. It consists of a programmable ESP32 module that converts the pulses from the Radiation Click module. This module, in the presence of ionizing radiation, detects gamma, beta, and x-rays using the BG51 sensor which is based on the operation of a custom PIN diode array. During the radioactive activity, the number of pulses is as dense as the radiation is high. To get the radiation dose corresponding to measurement during a time interval (in this case of the study we opted for one minute) the equation (1) is needed for the conversion. Multiply by 60 to obtain the number of pulses in one hour and $a=5\text{cpm}/\mu\text{Sv/h}$ is the sensitivity of the sensor [22].

$$Dose(\mu\text{Sv}) = \frac{60}{a}(\text{number of pulse (cpm)}) \quad (1)$$

The data collected per measurement is stored in the SD card for database building. The radiation dose level is displayed in real-time on the TFT LCD screen. The latter is responsible for presenting the radiation dose and the curve over time.

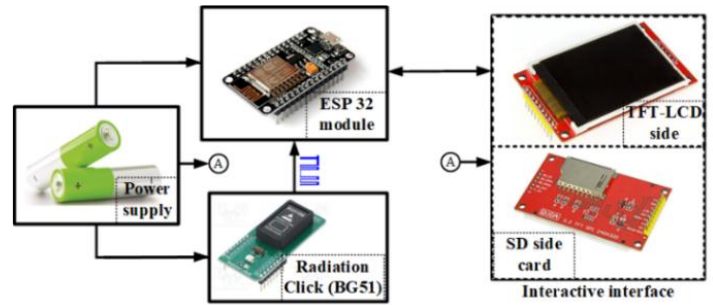


Fig 1. Synoptic of ionizing radiation measurement and user-module interaction.

Table 1. Hardware modules characteristics of the proposed instrument [21-22].




ESP32 (SOC device)		GENERAL CAPABILITIES	
		BASIC RESOURCES Dual cores 0 and 1 Clock frequency SRAM ROM memory Supported flash memory	CHARACTERISTICS Each core has 32 bits 80 -240 MHz 512 KB 448 KM Up to 32 Megabyte
		MAIN RESOURCES Build-in Wi-Fi module Build-in Bluetooth module 23 general purpose pins (real time reconfigurable by user code)	CHARACTERISTICS Std: 802.11, 2.2 -2.5GHz Version 4.2 (BLE) DIOs, 18ADC, 02DAC,16 PWM, 02 I ² S, 02 I ² S, Touch, etc. 10 01 02 01 01 Version 2.0 AP, Client, and Both Reset and enable 01
PINS FOR THE FRAMEWORK		ELECTRICAL AND THERMAL CHARACTERISTICS	
Pins	Role	Vcc supported	5V-3.3 V
GPIO 5	TFT_LED	Active voltage range	2 V 3.6 V
GPIO 13	INT in BG51	Operation temperature	-40°C to +125°C
GPIO 18	TFT_RESET	MAIN RESOURCES SIGNIFICATION PWR LED GREEN Power indication LD2 IND Radiation indicator LED PZ1 Buzzer Radiation indicator buzzer SW1 indicator Enable/disable indicator Number of pin 16 Use MIKROBUS	
GPIO 19	TFT_SCK		
GPIO 25	TFT_DC	PINS USED AND CHARACTERISTICS	
GPIO 21	TFT_MISO	GPIO 15	INT
GPIO 22	TFT_CS	Vcc	5V supply
GPIO 23	TFT_MOSI	GND	Ground
Vcc	5V supply	Detects beta, gamma radiation and X-rays,	High immunity to RF and electrostatic fields,
GND	Ground	Detector sensitivity: 5 cpm/ $\mu\text{Sv/h}$,	Linear response (-30°C to 60°C)
Radiation Click device 		CHARACTERISTICS	
		Display color	RGB color 65K
LCD TFT ILI9341 with SD Card module 		UGS	MAR2406
		Screen size	2.4 inches
		Type	TFT
		IC driver	ILI9341
		Resolution	320*240
		Interface module	8 bits parallel interface
		Supply voltage	3.3V-5V
		Operation temperature	-20°C to +60°C
		Integrated SD card module	
		Arduino compatible	

Table 1 describes the characteristics of the hardware modules used. The ESP32 module and the LCD screen are compatible with the Arduino IDE environment. To program the display in the Arduino environment, the following libraries are necessary: SPI.h (Serial Peripheral Interface) is a synchronous serial data protocol promotes fast communication of the microcontroller between one or more devices over short distances in master-slave mode. It uses three lines common to all devices: MISO (Master In Slave Out) is the slave line for sending data to master, MOSI (Master Out Slave In) is the master line for sending data to the devices, SCK (Serial Clock) is the line that synchronizes the transmission of data generated by the master. An additional pin named SS (Slave Select) can be added to enable or disable one of the peripherals;

Adafruit_GFX.h Arduino to provide a common syntax and set of graphical functions for all Adafruit LCD (Liquid Crystal Display) and OLED (Organic Light-Emitting Diode) displays and Adafruit_ILI9341.h allows to take into account the function of the display integrating a touch screen and a micro-SD card.

2.2. Methodologies

2.2.1. Schematic diagram of the new instrument

In Fig. 2, we show in the Proteus/ISIS environment simulation the electronic circuit of the ionizing radiation measurement prototype. It consists of all the electronic modules described in sub-section 2.1 and presented in table 1.

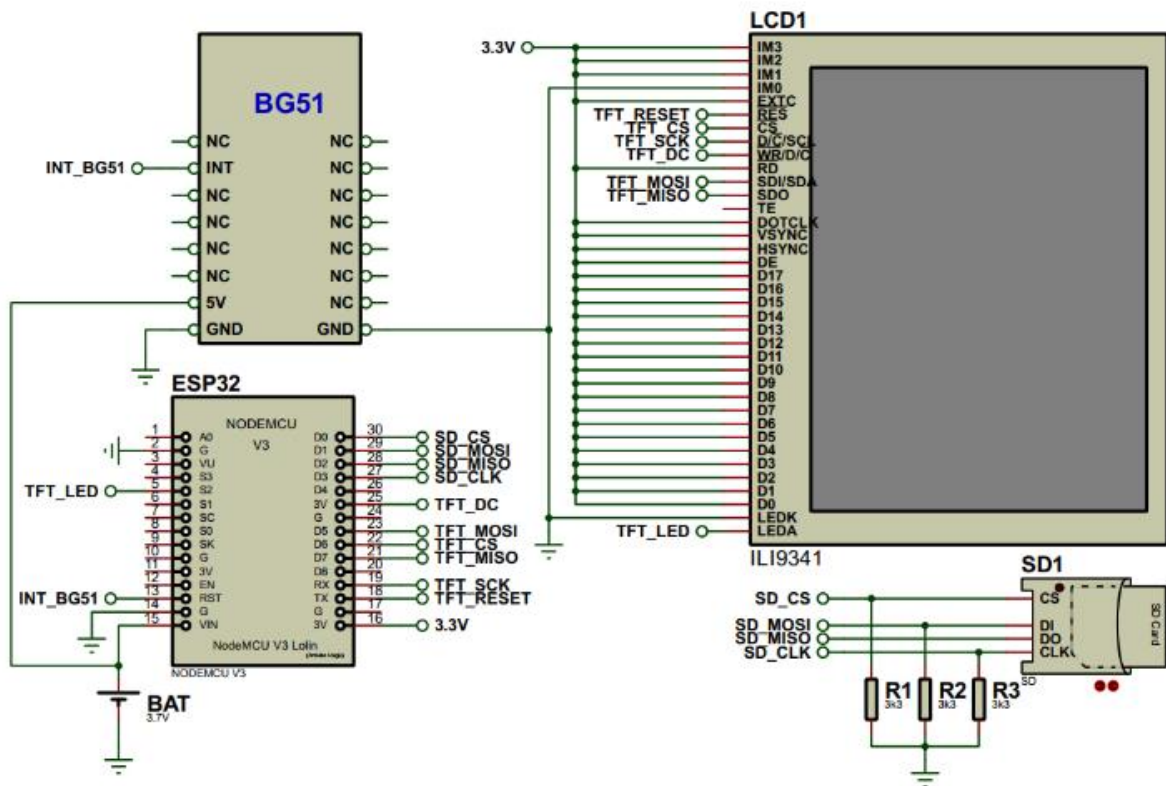


Fig 2. Electronic circuit of the proposed module in Proteus/ISIS environment

2.2.2 Digital signal acquisition and monitoring

To design the interface of the ionizing radiation acquisition module, we propose an architecture based on the flowchart in Fig. 3 whose subprograms are given in Figs.4, 5, 6. In Fig.2, the program imports all the libraries and libraries that reference the 2.4-inch TFT ILI934 LCD screen into the Arduino program editor. Three subroutines will be executed: the first one allows to define the area and the arc of the radiation dose indicator frame as described in Fig. 3. The second one allows drawing the gauge that allows indicating the number of pulses as described in Fig.5. The last subroutine allows representing the marker where the

ionizing radiation dose level will be plotted for fourteen minutes. This subroutine is described in Fig.6. The evaluation of the number of pulses is done for 10 seconds. However, the actual dose considered will be that of the preceding evaluation. After this time, the measured pulse number is changed back to the hour and the new ionizing radiation dose is calculated as described in equation (1). To

$$\begin{cases} x=0.00178*time+48 \\ y=-0.015*pulse_count+308 \end{cases} \quad (2)$$

represent a point in the curve over time, we propose the following equation to calculate the chord.

When the time variable accumulates 14 minutes, it is reset to zero and the marker is reset for a new trace. The data collected through the "count_pulse" counter can be stored

directly in the SD card to serve as a database. In the global operation, the subprograms are called when an indicator changes its position

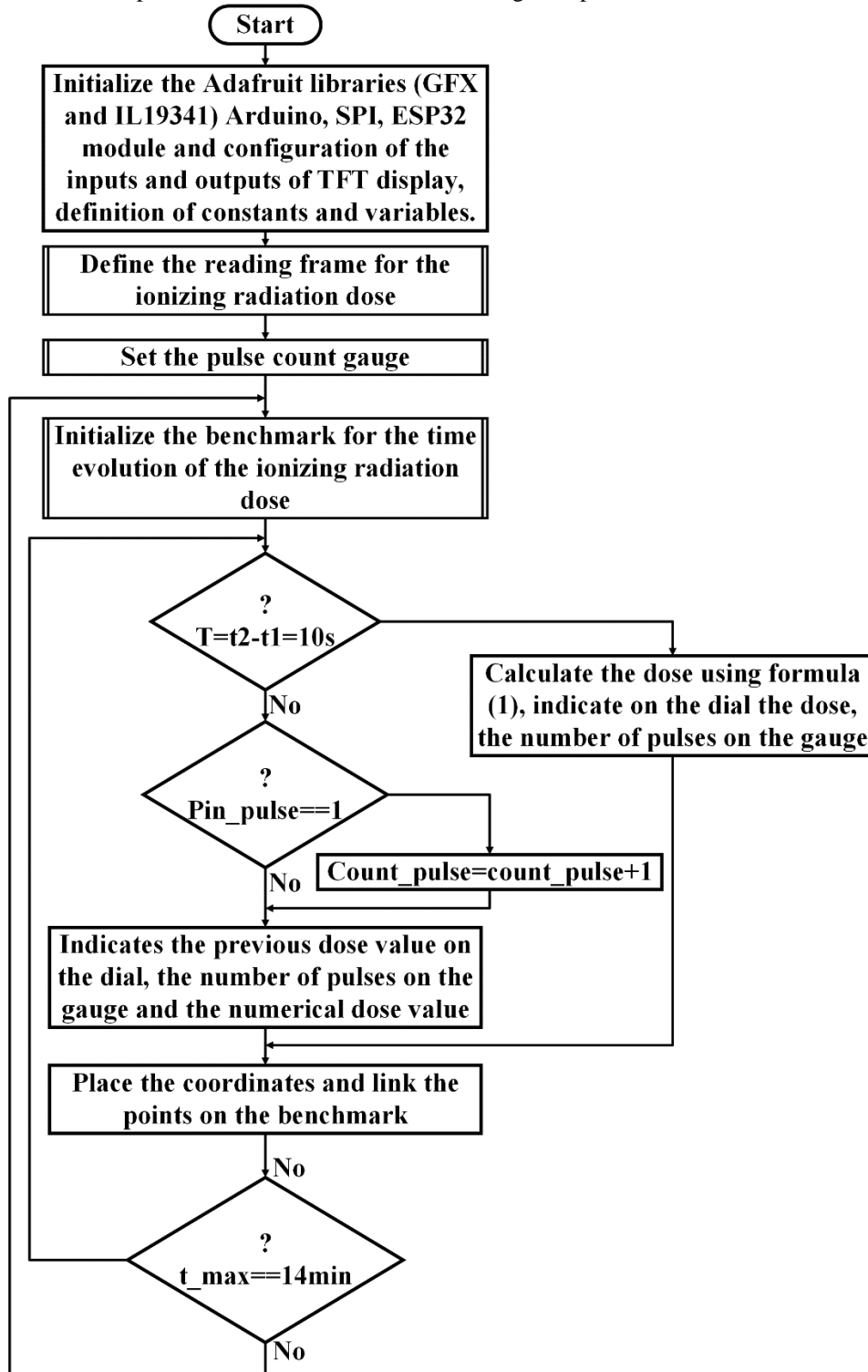


Fig. 3. Flowchart design of the data acquisition and collection program and display interface

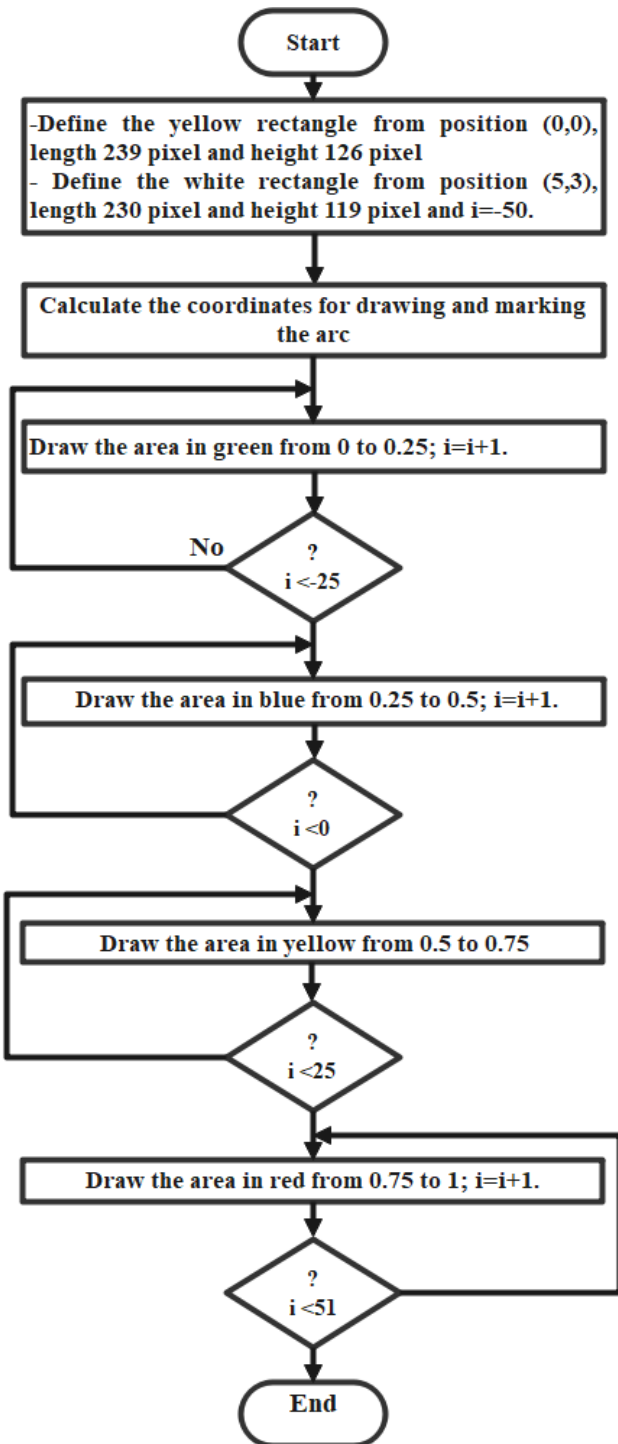


Fig 4. Flowchart of the frame for the indication of the ionizing radiation dose.

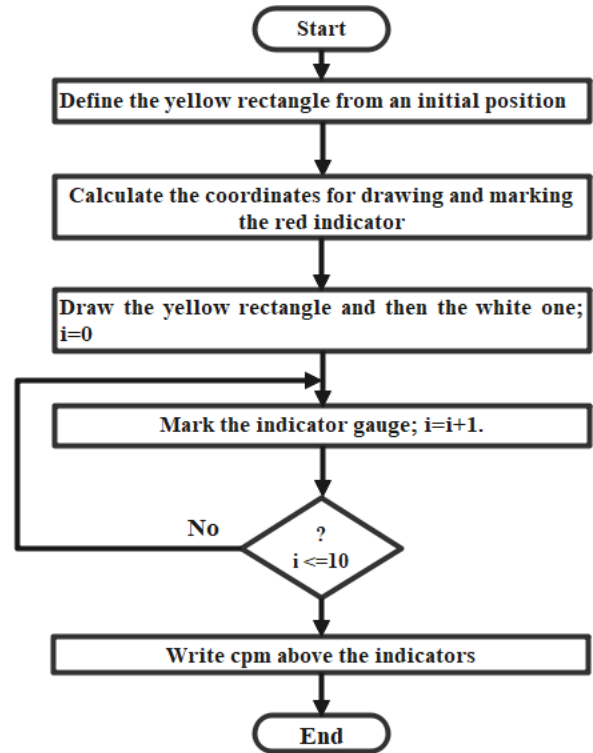


Fig 5. Flowchart design of the pulse count indicator gauge

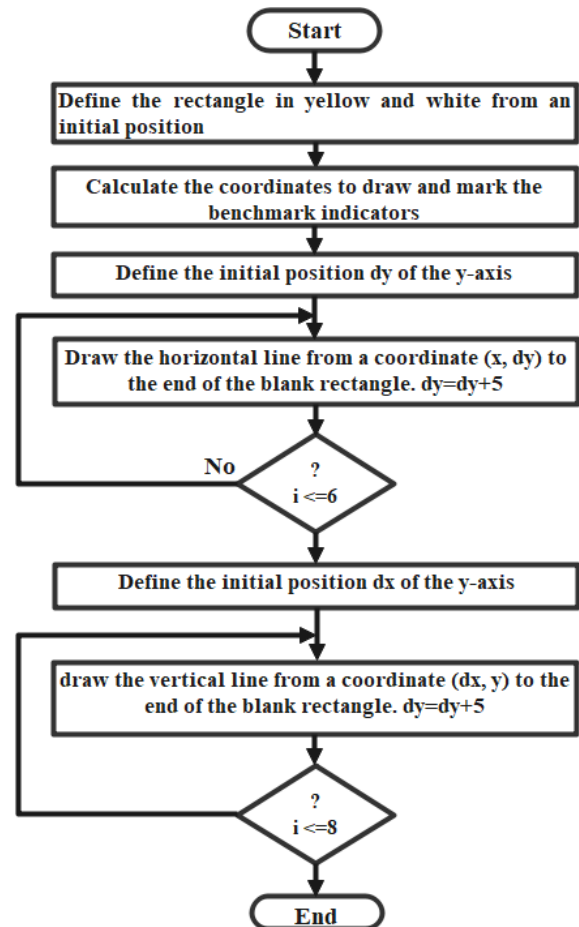
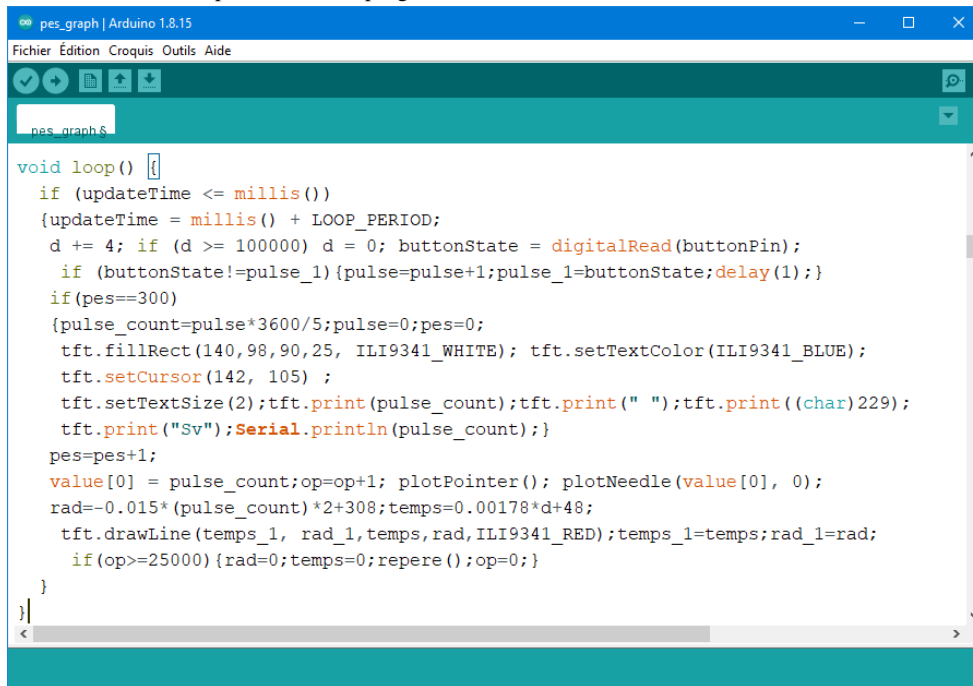


Fig. 6. Flowchart for drawing the benchmark

In Fig. 7 we present the main program of the flowchart of fig. 3 in the Arduino environment and the compilation of the program is

presented by the Windows window of Fig. 8 where we observe the program of the flowchart of Fig. 5.

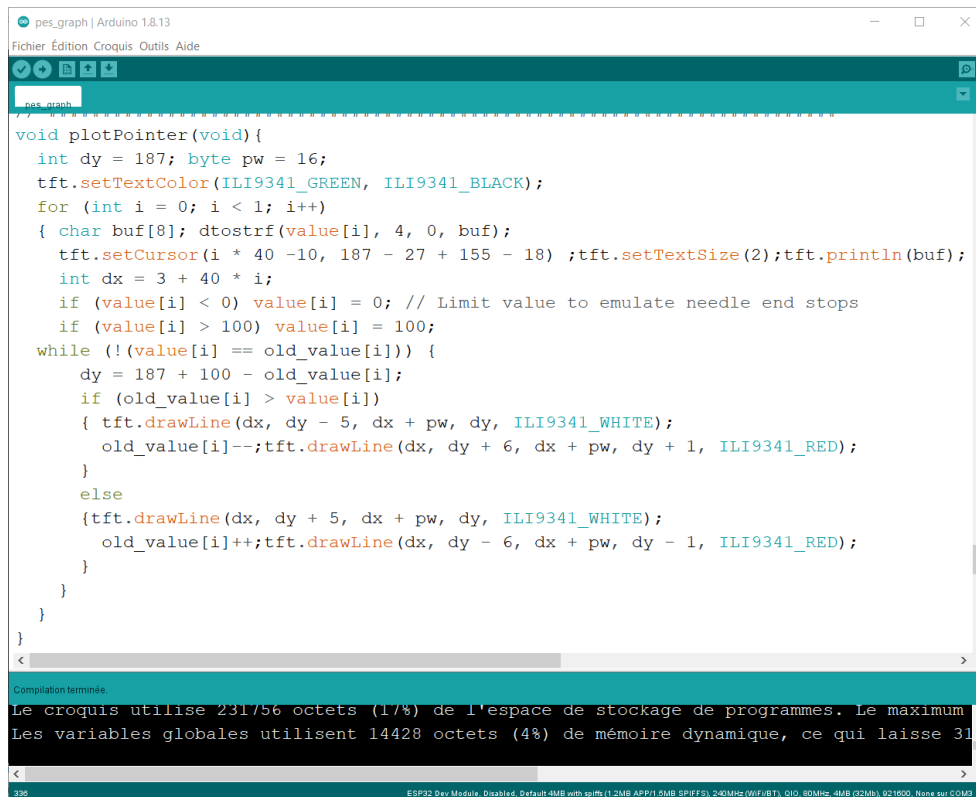


```

void loop() {
  if (updateTime <= millis())
  {updateTime = millis() + LOOP_PERIOD;
  d += 4; if (d >= 100000) d = 0; buttonState = digitalRead(buttonPin);
  if (buttonState!=pulse_1){pulse=pulse+1;pulse_1=buttonState;delay(1);}
  if(pes==300)
  {pulse_count=pulse*3600/5;pulse=0;pes=0;
  tft.fillRect(140,98,90,25, ILI9341_WHITE); tft.setTextColor(ILI9341_BLUE);
  tft.setCursor(142, 105) ;
  tft.setTextSize(2);tft.print(pulse_count);tft.print(" ");tft.print((char)229);
  tft.print("Sv");Serial.println(pulse_count);}
  pes=pes+1;
  value[0] = pulse_count;op=op+1; plotPointer(); plotNeedle(value[0], 0);
  rad=-0.015*(pulse_count)*2+308;temps=0.00178*d+48;
  tft.drawLine(temps_1, rad_1,temps,rad,ILI9341_RED);temps_1=temps;rad_1=rad;
  if(op>=25000){rad=0;temps=0;repere();op=0;}
}
}

```

Fig. 7. A view of the Arduino IDE/C++ framework of the main program presented by the flowchart in Fig.3.



```

void plotPointer(void){
  int dy = 187; byte pw = 16;
  tft.setTextColor(ILI9341_GREEN, ILI9341_BLACK);
  for (int i = 0; i < 1; i++)
  { char buf[8]; dtostrf(value[i], 4, 0, buf);
  tft.setCursor(i * 40 -10, 187 - 27 + 155 - 18) ;tft.setTextSize(2);tft.println(buf);
  int dx = 3 + 40 * i;
  if (value[i] < 0) value[i] = 0; // Limit value to emulate needle end stops
  if (value[i] > 100) value[i] = 100;
  while (!(value[i] == old_value[i])) {
    dy = 187 + 100 - old_value[i];
    if (old_value[i] > value[i])
    { tft.drawLine(dx, dy - 5, dx + pw, dy, ILI9341_WHITE);
      old_value[i]--;tft.drawLine(dx, dy + 6, dx + pw, dy + 1, ILI9341_RED);
    }
    else
    {tft.drawLine(dx, dy + 5, dx + pw, dy, ILI9341_WHITE);
      old_value[i]++;tft.drawLine(dx, dy - 6, dx + pw, dy - 1, ILI9341_RED);
    }
  }
}
}
}

```

Compilation terminée
Le croquis utilise 231/56 octets (1%) de l'espace de stockage de programmes. Le maximum
Les variables globales utilisent 14428 octets (4%) de mémoire dynamique, ce qui laisse 31

ESP32 Dev Module, Disabled, Default 4MB with spiffs (1.2MB APP/1.5MB SPIFFS), 240MHz (WiFi/BT), Q10, 80MHz, 4MB (Q2MB), 921600, None sur COM3

Fig. 8. Compilation window of the Arduino C++ sketch for the ES-32 microchip (view of the Arduino code in the flowchart of Fig.5).

2.3. Experimental Workbench and prototyping instrument strategy

The experimental bench that led to the results of section 3 is presented by Fig.9. It is composed of a computer (1) which allows to code and compile the algorithms presented in Fig. 3, 4, 5 and 6 in Arduino environment and to upload the program in the microcontroller. The display monitor (TFT LCD) is shown by (2), the BG 51 module for ionizing radiation acquisition is shown by (3). Its measurement range varies from 0.1 μ Sv/h to 100 μ Sv/h and corresponds to output pulses with periods ranging from 50 μ s to 200 μ s (5kHz to 20kHz) [22]. (4) represents the ESP 32 module and (5) the oscilloscope which allowed to check the effectiveness of the pulse.

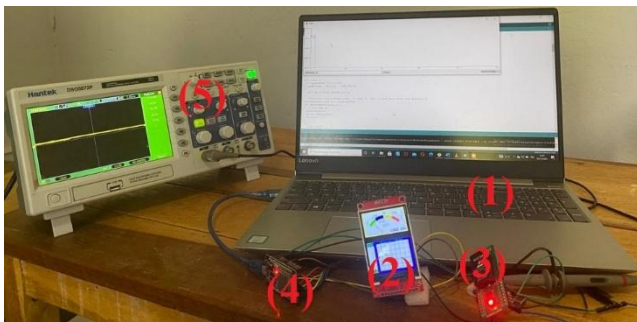


Fig 9. The experimental bench

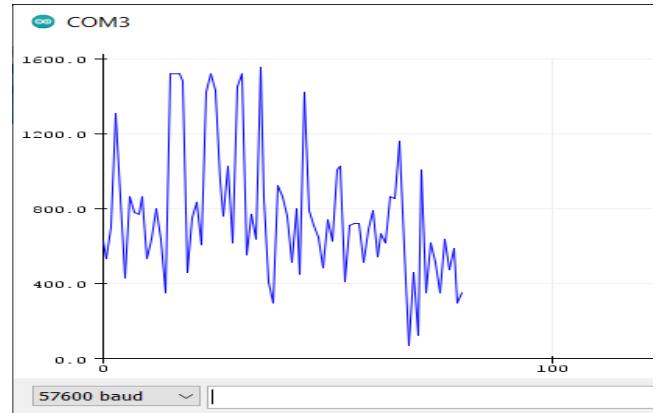
3. Results and Discussion

The experimental result obtained after the test in the laboratory of Higher Technical Teachers Training College of University of Yaoundé I in Ebolowa are presented in Fig. 10, 11 and 12. Dose measurements are made in the air in the first instance and in the second, we excite the sensor radiation of a Wi-Fi antenna placed near a phone in call emission. This operation excites the BG51 radiation sensor and creates an emulation of the ionizing wave environment. Fig 10 shows the behaviour of the output of the sensor module BG 51 during the emulation phase of this process.

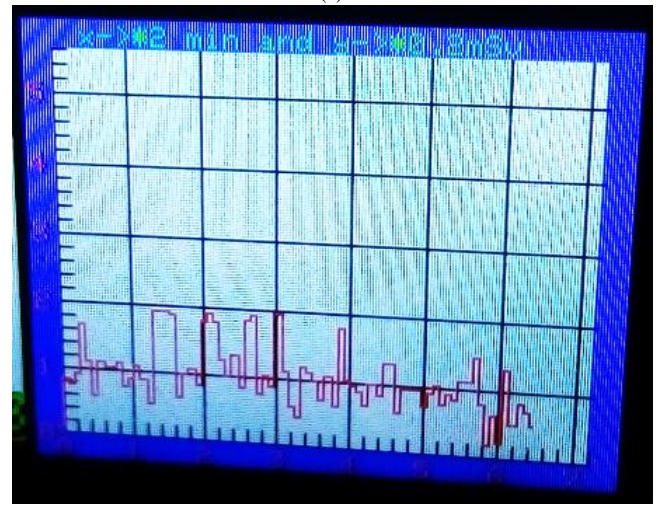


Fig 10. Output signal of the BG 51 module during the emulation phase.

The results in Fig.11 show the prototype in the validation phase in the Arduino programming environment. The plots are in micro-Sievert. We observe a similarity between the two curves of Fig. 11(a) and 11(b). this test validates the function and the quality of tracer to be reproduced in time that we have proposed.



(a)



(b)

Fig 11. Testing the prototype and the plotter through the Arduino environment: (a) Curve obtained with the tracer of Arduino environment; (b) Curve obtained with the tracer of the proposed protocol

The interface shown has a pulse-per-second gauge shown as (1) in Fig. 12(a). The ionizing radiation dose is indicated by a dial with the measured value multiplied by 10 as shown by (2) in Fig. 12(a). An additional numerical display option is present and is indicated by (3) in Fig. 12(a). A frame is reserved for the representation of the time evolution of the radiation dose in the air as indicated by (4) in Fig. 12(a). In Fig. 12(b), we present the results obtained in the measurement environment in the absence of radiation activity. During this phase, the ionizing radiation measurement is very low and can vary in time despite the presence of a peak around 7. The time scale is in minutes and one division corresponds to two (2) minutes on this scale. On the y-axis, one division corresponds to 0.4mSv. The proposed measurement interface around the ESP32 card shows the measurements obtained during an ionizing

radiation activity in Fig. 12(c). This figure shows a well-varying radiation activity over time. The number of samples represented by the graph is 25,000 or

approximately 30 samples in one second.

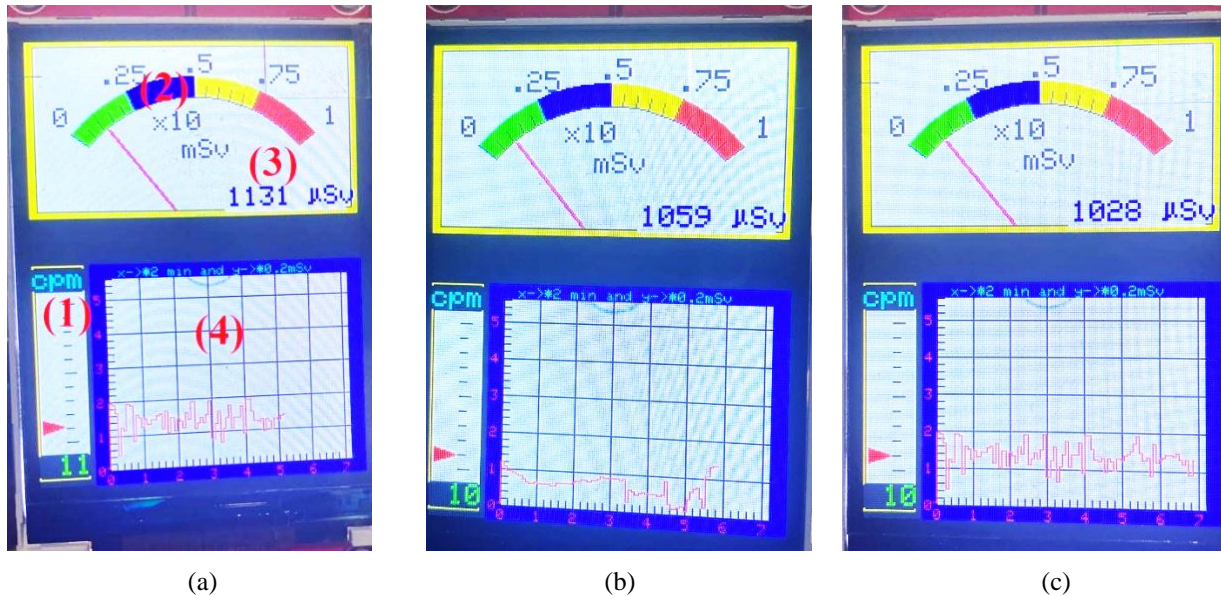


Fig 12. Results of the proposed measurement prototype

4. Conclusion

The work that was carried out in this paper was to present a digital biomedical electronic instrument for biomedical imaging personnel exposed to high radiation risks. We have reviewed the different means of protection and measurement technologies available in the literature. Based on the identified limitations, we proposed a digital ionizing radiation measurement device with an oscilloscope option for medical imaging personnel. The ESP32 card combined with a radiation click module equipped with a BG51 sensor allows the measurement of the radiation dose in the air.

The results of the measurement are indicated through a 2.4 inch TFT display with indicators such as gauge, needle dial, and graph. Our main contributions were to introduce an expert system capable of measuring, collecting data, analyzing, and alerting the operator or medical imaging technician of an overdose. The future work in this study will be to miniaturize the prototype if necessary and to make the communication interface multitasking and multi-measuring across several technicians.

Conflict of Interest

The authors declare that they have no conflict of interest

References

1. Brown N, Jones L. Knowledge of medical imaging radiation dose and risk among doctors. *Journal of medical imaging and radiation oncology*. 2013, 57(1): 8-14. <https://doi.org/10.1111/j.1754-9485.2012.02469.x>
2. Etard C, Sinno-Tellier S, Aubert B. Exposition de la population française aux rayonnements ionisants liée aux actes de diagnostic médical en 2007. *Ints Veille Sanit*. 2010.
3. De Graaf P, Gröricke S, Rodjan F et al. Guidelines for imaging retinoblastoma: imaging principales and MRI standardization. *Pediatr Radiol*. 2012; 42:2-14. <https://doi.org/10.1007/s00247-011-2201-5>
4. Street LJ. Introduction to biomedical Engineering technology (3rd ed.) *CRC press*. 2016. <http://doi.org/10.1201/9781315370804>
5. Guy C, Ffytche D, An introduction to the principles of medical imaging. *Imperial College Press*. 2005.
6. Ammerich M. Les effets des rayonnements sur l'être humain: est-ce que ça mal docteur?: la radioactivité sous surveillance: Et autres notions en radioprotection. Les Ulis: EDP Sciences. 2021: 28-40. <https://doi.org/10.1051/978-2-7598-0992-9-005>
7. Kis D, Persa E, Szatmari T, Antal L, Bota A, Csorda Ibarbara, Hargitai R, Jezso B, Kis E, Mihaly J, et al. The effect of ionising radiation on the phenotype of bone marrow-derived extracellular vesicles. *Br. J. Radiol*. 2020: 20200319, 93(1115).

<http://doi.org/10.1259/bjr.20200319>.

8. Francky K. B. S, D. Henri, Euloge B. T, O. Moise, Timothée M. Connaissances des Prescripteurs en Radioprotection des Patients en Centrafrique. *Eur. Sci. J. ESJ*. 2019 : 15(12). <http://doi.org/10.19044/esj.2019.v15n12p1>.
9. Ongolo-Zogo P, Nguehouo MB, Yomi J, Nko'o Amven S. Connaissances en matière de radioprotection : enquête auprès des personnels des services hospitaliers de radiodiagnostic, radiothérapie et médecine nucléaire à yaoundé-Cameroun. *Radioprotection*. 2013, 48(1), 39-49. <http://doi.org/10.1051/radiopro/2012017>
10. Blkissou AD, Pefura-yone EW, Endale Mangamba LM, Onana Ngono I, Poka Mayap V, Evouna Mbarga A, Assamba Mpom SA, Kanko NF, Fodjeu G, Tagne Kamdem PE, Fogang D, Kuaban C. Residual pleural opacity in patients treated for pleural tuberculosis in Yaounde. *Revue de pneumologie clinique*. 2015, 72(2), 115-121. <http://doi.org/10.1016/j.pneumo.2015.09.004>
11. Leclerc JC, Beregi JP. Quality in radiology and medical imaging : State of art. *Journal d'imagerie diagnostique et interventionnelle*. 2019, 2(2), 114-117. <https://doi.org/10.1016/j.jidi.2019.01.006>
12. Lévêque L, Bosmans H, Cockmartin L, Liu H. State of the art : Eye-tracking studies in medical imaging. *IEEE Access*. 2018, 6, 37023-37034. <http://doi.org/10.1109/ACCESS.2018.2851451>
13. Kombaev TSh, Artemov ME, Zefirov IV. Designing radiation protection for the scientific equipment complex of the earth's remote sensing spacecraft. *Engineering journal: Science and innovation*. 2019, 5(89). Doi:10.18698/2308-6033-2019-5-1878
14. Laal M, Innovation process in medical imaging. *Procedia-Social and Behavioral Sciences*, 2013, 81: 60-64. <https://doi.org/10.1016/j.sbspro.2013.06.388>
15. Bottollier-Depois JF, Clairand I, Donadille L, Rannou A. Dosimétrie individuelle pour l'irradiation externe : évolution des pratiques et des techniques. *Radioprotection*, 2007, 42(4): 477-487. <http://doi.org/10.1051/radiopro:2007033>
16. Salomaa S, Jourdain JR, Kreuzer M, Jung T, Repussard J. Multidisciplinary European low dose initiative: an update of the MELODI program. *International Journal of Radiation Biology*. 2017, 93(10): 1035-1039. <https://doi.org/10.1080/09553002.20017.1281463>
17. Paulo G, Damilakis J, Tsapaki V et al. Diagnostic reference levels based on clinical indication in computed tomography: a literature review. *Insights Imaging*. 2020, 11(96). <https://doi.org/10.1186/s13244-020-00899-y>
18. Akber AA, Wiggins MB. A Review of Dose Rate Meters as First Responders to Ionising Radiation. *J. Radiat. Prot. Res.* 2019, 44(3): 97-102. <http://doi.org/10.14407/jrpr.2019.44.3.97>
19. Garcia-Sanchez AJ, Angosto EAG, Riquelme PAM, Berna AS. Ionizing radiation measurement solution in a hospital environment. *Sensors*. 2018;510, 18(2). <https://doi.org/10.3390/s18020510>
20. Mbarndouka Taamté J, Kountchou Noubé M, Bodo B, Tchunte Siaka YF, Nducol N, Folifack Signing VR, Tagne Mogue RL, Saïdou. International Journal of Energy and Environmental Engineering. 2021. <https://doi.org/10.1007/s40095-021-00415-y>
21. Owoundi Etouké P, Nneme Nneme L, Mbihi J. ESP32-Based Workbench for Digital Control Systems of Duty-Cycle Modulation Buck Choppers. *International Journal of Scientific Research in Computer Science and Engineering*. 2020, 8(6): 62-67
22. Radiation Click. Radiation Click 4036 radiation is a click board based on BG51 radiation sensor. available on-line 21 September 2021 in <http://www.mikroe.com/radiation-click>.

Recommended Citation

Emvoutou Ndongo S, Mbihi J, Ngo Bissé JT, Nguemgne Malongte C. Study and experimental prototyping of a digital instrument for detection and acquisition with local monitoring on LCD of ionizing radiations using BG51 module and ESP32 microchip. *Alger. J. Eng. Technol.* 2021, 5:55-63. <http://dx.doi.org/10.5281/zenodo.5717122>



This work is licensed under a [Creative Commons Attribution-NonCommercial 4.0 International License](https://creativecommons.org/licenses/by-nc/4.0/)